ON A QUASILINEAR DEGENERATE HYPERBOLIC SYSTEM OF CONSERVATION LAWS DESCRIBING NONLINEAR ADVECTION PHENOMENA

LING HSIAO AND PIERO DE MOTTONI

ABSTRACT. We consider a two-dimensional system of conservation laws which is hyperbolic but degenerate, for either characteristic field is genuinely nonlinear in one half of the phase-plane and linearly degenerate in the other half. We prove the existence and uniqueness of the solution of the Riemann problem and the existence of a (BV) solution of the initial-value problem. This system arises in modelling certain nonlinear advection processes and, as shown by the support properties we establish in case of special initial data, may describe pattern differentiation.

0. Introduction. The object of the present paper is to study the system of conservation laws

$$(0.1) \qquad \begin{bmatrix} u_t + (u(1-v))_x = 0 \\ v_t + (v(1+u))_x = 0 \end{bmatrix} \text{ in } \mathbf{R} \times \mathbf{R}^+.$$

This system arises if we consider u, v as the space derivatives of non-negative quantities representing the densities of two populations, the *fugitives* (denoted by $U(x,t)$) and the *pursuers* (denoted by $V(t,x)$). According to a model originally proposed by Murray and Cohen [**12**], we may characterize a pursuing-escape interaction with predation along a straight line course by the equations

$$(0.2) \qquad \begin{bmatrix} U_t + (U(1-V_x))_x = -UV_{xx}, \\ V_t + (V(1+U_x))_x = VU_{xx}, \end{bmatrix}$$

where units have been renormalized and it is assumed that, in the absence of interaction, the two populations run with the same velocity, -1. The following features are incorporated into this model, where only the total mass of the two populations $\int (U+V) \, dx$ is conserved:

(i) Since $1 - V_x$, $1 + U_x$ represent the advection velocities of the U's, respectively of the V's, the fugitives provoke the pursuers into the pursuing action by moving away, and the pursuers cause the fugitives to escape by running after them: indeed, the U's escape from the V's at a rate proportional to the space gradient of the V's and, in turn, the V's try to approach the U's at a rate proportional to the space gradient of the U's.

(ii) The terms on the right-hand side account for a switching predation mechanism governed by the relative space profiles of the population distributions: the fugitives are eaten by the pursuers' forerunners which reach them (indeed, at points where the V-slope is increasing from negative values to zero), but react against any group of pursuers (decreasing V-slope) by eating the pursuers whenever such a group tries to overtake them. In turn, the pursuers feed on the fugitives' rearguard (increasing U-slope), but are eaten by the fugitives as soon as they attempt to attack a group of them (decreasing U-slope).

It is tempting to consider system (0.1) with *different* linear advection velocities (say, with 1 replaced by a constant $a \neq 1$ in either of the equations in (0.1)); this, however, leads to a mixed-type system of quite involved nature, which we will not investigate here.

System (0.1) is hyperbolic, but not strictly hyperbolic, since its characteristic speeds coincide at $u = v$ (for general facts about hyperbolic conservation laws and for the basic properties of the solutions we are going to work with, see Section 1 below). Moreover, for each i $(i = 1, 2)$, the i-th characteristic field is genuinely nonlinear in one half of the phase-plane ($u < v$ for $i = 1$, $u > v$ for $i = 2$), and linearly degenerate in another half ($u > v$ for $i = 1$, $u < v$ for $i = 2$). Because of these nonstandard features one might wonder whether the known entropy criteria are sufficient to single out a unique "physically reasonable" (weak) solution of the Riemann problem (within the class of the *bounded variation* functions (BV). Indeed, we shall show that, by naturally extending the Lax entropy condition to cover contact discontinuities, a unique solution for the Riemann problem can be shown to exist. This will be done in Section 2. Another feature of the system (0.1) is that shock and rarefaction curves coincide (other, different systems sharing this property have been considered in the literature, in connection with various models in applied sciences—see, e.g., [**1, 5, 6, 7, 11, 13, 14**]. This feature in our model simplifies the structure of

the solutions of the Riemann problem and of the wave interaction and makes it possible to solve the Cauchy problem for arbitrary data of bounded variation, as it will be explained in Section 3. In Section 4 a special Cauchy problem will be solved, showing that an initial condition in which the U's and the V's have the *same* space distribution evolves, after a finite time, into traveling waves in which the initial symmetry is broken down, for the two components have markedly *different* space structures. This suggests that our equations could be used as a model in processes describing pattern differentiation.

1. Basic facts about hyperbolic conservation laws and first properties of the solutions. In the first place, (0.1) being of the form

$$(1.1) \qquad U_t + (F(U))_x = 0 \quad \text{with} \quad U = (u, v)^T,$$

is a system of hyperbolic conservation laws: the i-th eigenvalue of the Jacobian $DF(U)$ of $F(U)$ evaluated at a solution (u, v) will be referred to as the *i-th characteristic speed* of (u, v), $i = 1, 2$. As usual, we stipulate

$$\lambda_1(u, v) \leq \lambda_2(u, v).$$

We shall denote by r_i the associated (right) eigenvector. An easy calculation shows that, in our case,
(1.2)
$$\lambda_1 = \begin{cases} 1 + u - v & \text{when } u < v \\ 1 & \text{when } u > v \end{cases}, \quad r_1 = \begin{cases} (1, -1)^T & \text{when } u < v \\ (u, -v)^T & \text{when } u > v, \end{cases}$$

whereas
(1.3)
$$\lambda_2 = \begin{cases} 1 + u - v & \text{when } u > v \\ 1 & \text{when } u < v \end{cases}, \quad r_2 = \begin{cases} (1, -1)^T & \text{when } u > v \\ (u, -v)^T & \text{when } u < v. \end{cases}$$

An *i-th rarefaction wave* for (1.1), $i = 1, 2$, is a (smooth, single-valued) similarity solution $u = u(\xi)$, $v = v(\xi)$, where $\xi = x/t$ such that the i-th characteristic speed is increasing in ξ. Denoting by $\prime$ the derivative with respect to ξ, a rarefaction wave (u, v) is, therefore, characterized by

$$(\xi I - DF(U))U' = 0;$$

thus ξ has to be a characteristic speed λ_i, and the solution's slope du/dv in the phase-plane is given by the associated (right) eigenvector. The equation $du/dv = r_i(u,v)$ defines the *i-th rarefaction curve* R_i, $i = 1, 2$.

In our case, taking into account the above values of λ_i, r_i, we conclude that a (single-valued, smooth) function $(u(\xi), v(\xi))$ is a 1-*rarefaction wave* relative to (1.1), if

$$
(1.4) \qquad \begin{aligned} \xi &= 1 + u - v \\ u + v &= \text{const.} \end{aligned}
$$

on some interval $(\xi_1, \xi_2) \subset (-\infty, 1)$. The associated 1-rarefaction curve R_1 should be given by $du/dv = -1$ as $u < v$, $du/dv = -u/v$ as $u > v$, i.e.,

$$
(1.5) \quad R_1 : \begin{cases} u + v = \text{ const. as } u < v, & \text{along which } \lambda_1 \text{ increases} \\ & \qquad\qquad \text{as } u \text{ increases,} \\ uv = \text{ const. as } u > v, & \text{where } \lambda_1 \equiv 1. \end{cases}
$$

Since λ_1 is constant on the branch $uv = \text{ const.}$ of the R_1-curve, it is clear that only the part $v > u$ on R_1 provides the 1-rarefaction wave (which we shall still denote by R_1).

Likewise, $(u(\xi), v(\xi))$ is a 2-*rarefaction wave* relative to (1.1) if (1.4) holds on some interval $(\xi_1, \xi_2) \subset (1, \infty)$. To obtain the associated 2-rarefaction curve R_2, let us integrate $du/dv = -1$ for $u > v$, and $du/dv = -u/v$ for $u < v$, which yields

$$
(1.6) \quad R_2 : \begin{cases} u + v = \text{ const. as } u > v, & \text{along which } \lambda_2 \text{ increases} \\ & \qquad\qquad \text{as } u \text{ increases,} \\ uv = \text{const. as } u < v, & \text{where } \lambda_2 \equiv 1. \end{cases}
$$

Again, only the part $u > v$ on R_2 provides the 2-rarefaction curve, which we shall still denote by R_2.

Let us now turn to *discontinuous solutions*. They are characterized by the left-hand, respectively right-hand, values at the discontinuity, and by the discontinuity's speed, σ. These quantities are related among
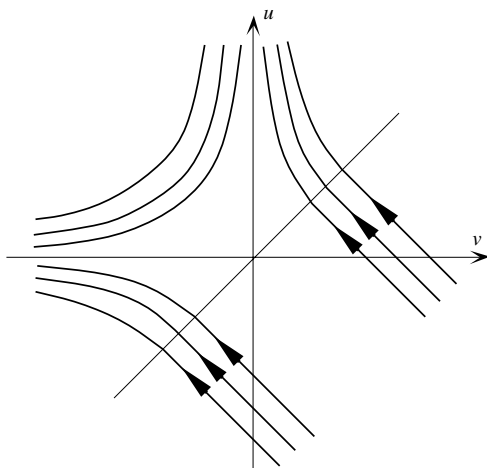
FIGURE 1.1.1. The R_1-curves (1-rarefaction curves only for $u < v$).
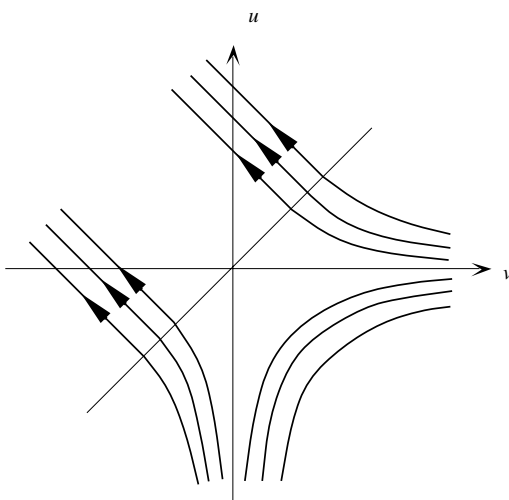

FIGURE 1.1.2. The R_2-curves (2-rarefaction curves only for $u > v$).

them by the well-known *Rankine-Hugoniot* conditions which, in the present case, take on the form

$$
(1.7) \qquad
\begin{bmatrix}
\sigma[u] - [(1-v)u] = 0 \\
\sigma[v] - [(1+u)v] = 0,
\end{bmatrix}
$$

where $[w] = w_r - w_\ell$ denotes the *jump* of the quantity w across the discontinuity. Note that, eliminating σ from (1.7), we obtain $[uv]([u] + [v]) = 0$, which implies that, for fixed values (u_0, v_0) of the left-hand values, the right-hand values (u, v) satisfy

$$
(1.8) \qquad \text{either} \quad uv = u_0 v_0 \quad \text{or} \quad u + v = u_0 + v_0.
$$

Furthermore, on $uv = u_0 v_0$ we have $\sigma = 1$, while on $u + v = u_0 + v_0$ we have $\sigma = 1 + u - v_0$.

To introduce the *entropy condition*, denote, by $\lambda_{i\ell} = \lambda_i(u_\ell, v_\ell)$, $i = 1, 2$, the characteristic speeds evaluated at the left-hand value (u_ℓ, v_ℓ) of the discontinuity, and, by $\lambda_{ir} = \lambda_i(u_r, v_r)$, the characteristic speeds at the right-hand value (u_r, v_r) of the discontinuity.

According to the *Lax entropy condition* we shall say that a discontinuity with distinct values from the left and from the right (u_ℓ, v_ℓ), (u_r, v_r) is a *1-shock wave* or a *back shock wave* if its speed σ satisfies

$$
(1.9) \qquad \lambda_{1r} < \sigma < \lambda_{1\ell}, \qquad \sigma < \lambda_{2r},
$$

whereas it is a *2-shock wave* or a *front shock wave* if its speed σ satisfies

$$
(1.10) \qquad \lambda_{1\ell} < \sigma, \qquad \lambda_{2r} < \sigma < \lambda_{2\ell}.
$$

It will be convenient to impose a similar condition even for discontinuities whose speed equals one of the characteristic speeds—the so-called *contact discontinuities*. Thus, we shall say that a discontinuity is a *T-wave* if its speed σ satisfies either

$$
(1.11) \qquad \lambda_{1r} \le \sigma \le \lambda_{1\ell}, \qquad \sigma \le \lambda_{2r},
$$

or

$$
\lambda_{1\ell} \le \sigma, \qquad \lambda_{2r} \le \sigma \le \lambda_{2\ell}.
$$

In the following, we shall consider only discontinuities that are shock waves or T-waves.

Let us now investigate which kind of discontinuities can arise once the left-hand state (u_0, v_0) is specified. To this end, we refer to (1.8) which, as noted, characterizes the two possible curves on which the right-hand state (u, v) can lie; more specifically, recalling the expressions (1.2), (1.3) for $\lambda_i(u, v)$, we see that

(1) For any given state (u_0, v_0) in the (u, v)-plane with $u_0 > v_0$, along the curve $u + v = u_0 + v_0$, the quantity σ equals $1 + u - v_0$ and decreases from $\sigma > 1$ to $\sigma = 1$ as u decreases from u_0 to v_0; moreover, the entropy condition (1.10) is satisfied: for $u < v_0$, σ is still decreasing as u decreases, $\sigma < 1$, and the entropy condition (1.9) is fulfilled. Thus, we have a 2-shock wave with (u_0, v_0) as left state and (u, v) as right state, whenever (u, v) lies on $u + v = u_0 + v_0$ with $u_0 > u > v_0$, and a 1-shock wave if (u, v) lies on the same curve and $u < v_0$ (see Figure 1.2.1–1.2.6).

(2) For any given state (u_0, v_0) in the (u, v)-plane with $u_0 < v_0$, along the curve $u + v = u_0 + v_0$, the quantity σ equals $1 + u - v_0$ and decreases from $\sigma < 1$ as u decreases from u_0; moreover, the entropy condition (1.9) is satisfied. Thus we have a 1-shock wave with (u_0, v_0) as left state and (u, v) as right state whenever (u, v) lies on $u + v = u_0 + v_0$ with $u_0 > u$ (see Figure 1.3.1–1.3.3).

(3) For any given state (u_0, v_0) in the (u, v)-plane, along the curve $uv = u_0 v_0$ we have in any case a contact discontinuity; however, T-waves are not allowed to cross the $u = v$-line from $\{u < v\}$ to $\{u > v\}$.

2.

2a. *Riemann problem: existence and uniqueness.* Consider (0.1) with the following initial data

$$(2.1) \qquad (u, v)|_{t=0} = \begin{cases} (u_-, v_-) & \text{for } x < 0, \\ (u_+, v_+) & \text{for } x > 0, \end{cases}$$

where (u_-, v_-), (u_+, v_+) are arbitrary states in the (u, v)-plane. Since both the system (0.1) and the initial data (2.1) are invariant under the transformation $x \to \alpha x$, $t \to \alpha t$, we look for similarity solutions $u = u(\xi)$, $v = v(\xi)$, where $\xi = x/t$.
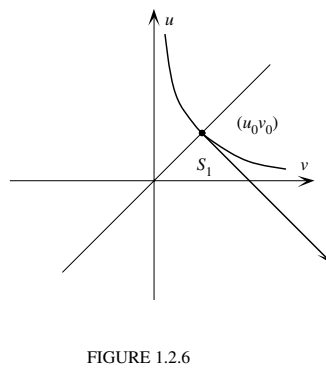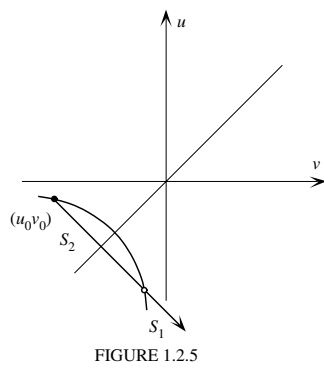
FIGURE 1.2.1

FIGURE 1.2.2

FIGURE 1.2.3

FIGURE 1.2.4

FIGURE 1.2.5

FIGURE 1.2.6

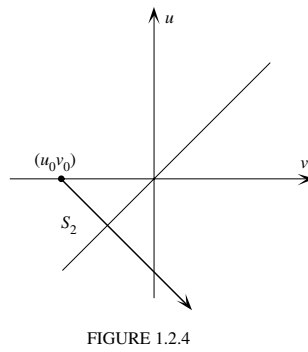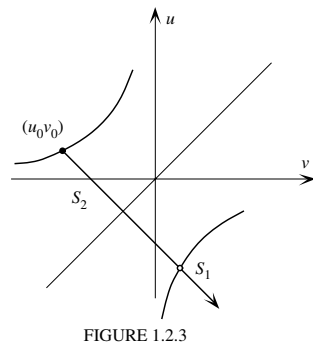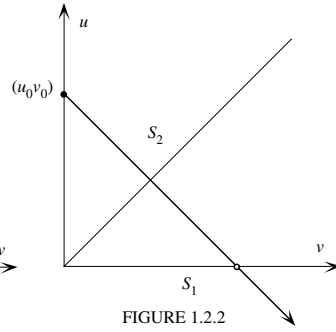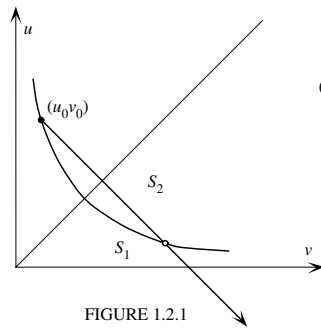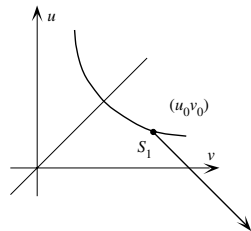FIGURE 1.2. Shock waves emanating from (u_0, v_0), $u_0 > v_0$.

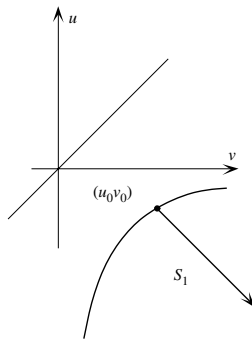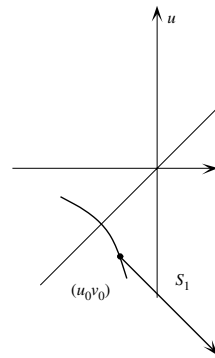FIGURE 1.3.1   FIGURE 1.3.2   FIGURE 1.3.3

FIGURE 1.3. Shock waves emanating from (u_0, v_0), $u_0 < v_0$.

Definition 2.1. A single-valued function $(u(\xi), v(\xi))$ is called an *admissible weak solution* of (0.1), (2.1) if

(i) It satisfies the boundary conditions $(u, v) \to (u_\pm, v_\pm)$ as $\xi \to \pm\infty$;

(ii) It is either a rarefaction wave or a constant state wherever it is smooth;

(iii) Any discontinuity satisfies the Rankine-Hugoniot condition (1.7); moreover, any shock satisfies either (1.9) or (1.10), and any contact discontinuity satisfies (1.11).

For given (u_-, v_-), consider the state (u, v) which can be joined to (u_-, v_-) on the right by either a 1-rarefaction wave, or a 1-shock or a T-wave. All such states form a curve, which will be called the *first wave curve* or *back wave curve*, $W_1(u_-, v_-)$.

First case. Let us first consider the case $0 < v_- < u_-$. The first wave curve consists of the whole curve $uv = u_- v_-$ through (u_-, v_-) and a part of the curve $u + v = u_- + v_-$ for $u < v_-$ (see Figure 2.1). Take any point $(\hat{u}, \hat{v}) \in W_1(u_-, v_-)$ and consider all the states that can be joined to $(\hat{u}, \hat{v})$ on the right by either a 2-rarefaction wave or a 2-shock or a T-wave. These states form another curve, called the *second wave curve* or *front wave curve*, $W_2(\hat{u}, \hat{v})$. Since each point on the branch
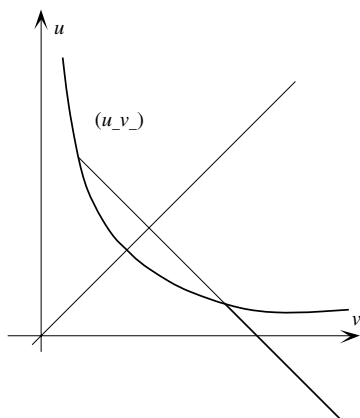
FIGURE 2.1. Candidates for the first wave curve W_1.

$uv = u_-v_-$, for $u < v_-$, has the same $W_2(\hat{u}, \hat{v})$ as $(\hat{u}, \hat{v}) = (v_-, u_-)$, we may neglect this branch, and, as first wave curve $W_1(u_-, v_-)$, we shall take the curve

$$\left[\begin{array}{ll} u + v = u_- + v_-, & \text{for } u \leq v_- \\ uv = u_-v_-, & \text{for } u > v_- \end{array}\right. \qquad \text{(see Figure 2.2)}.$$

Now consider the set of all the $W_2(\hat{u}, \hat{v})$ curves as the point $(\hat{u}, \hat{v})$ varies on $W_1(u_-, v_-)$. The existence and uniqueness for the Riemann problem (0.1), (2.1) is established if we can show that this set of curves covers the whole (u, v)-plane univalently. This will be precisely our program in the present section.

Subcase 1.1. In the first place, let us take any point $(\hat{u}, \hat{v})$ on $W_1(u_-, v_-)$, for $0 \leq \hat{u} \leq v_-$, and consider the curve $W_2(\hat{u}, \hat{v})$. There is just one choice for this curve, given by

$$\left[\begin{array}{l} uv = \hat{u}\hat{v}, \text{ for } u \leq \sqrt{\hat{u}\hat{v}}, \\ u + v = 2\sqrt{\hat{u}\hat{v}}, \text{ for } u > \sqrt{\hat{u}\hat{v}} \end{array}\right. \qquad \text{(see Figure 2.3)}.$$

(At first sight, one could think of another possible candidate for $W_2(\hat{u}, \hat{v})$, namely, the whole curve $uv = \hat{u}\hat{v}$; however, this curve violates
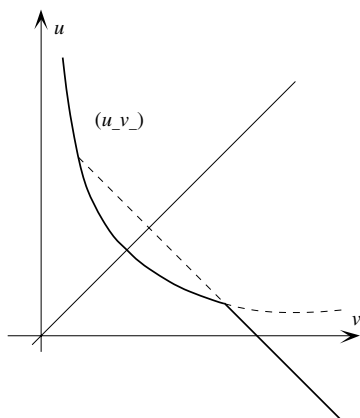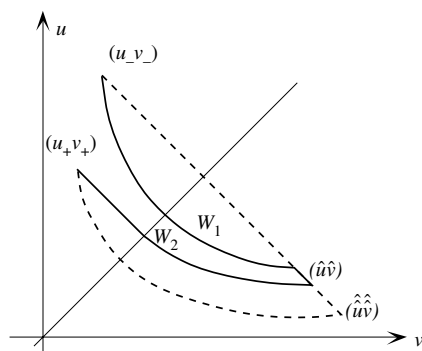
FIGURE 2.2. The *true* W_1 curve.

FIGURE 2.3. From $(\hat{u}, \hat{v})$ to (u_-, v_-) : the second wave curve (admissible: solid, inadmissible: dotted).

the condition (1.11) insofar as it crosses the $u = v$ line and, therefore, is not an admissible T-wave).

It is easy to show that, as $(\hat{u}, \hat{v})$ varies on $W_1(u_-, v_-)$ from $u > 0$ to $u \le v_-$, then the set $\{W_2(\hat{u}, \hat{v})\}$ covers univalently the domain

$$\{0 < u + v \le 2\sqrt{\hat{u}\hat{v}}, u > 0\} \cup \{uv \le u_-v_-, 0 < u < v\}$$

(see Figure 2.4).

Subcase 1.2. Next consider the case $(\hat{u}, \hat{v}) \in W_1(u_-, v_-)$ with $v_- < \hat{u} \le \sqrt{u_-v_-}$. Reasoning as in the previous case, it is easy to prove that the admissible second wave curve $W_2(\hat{u}, \hat{v})$ is just one, and it is defined by

$$\begin{cases} uv = \hat{u}\hat{v}, & \text{for } u \le \sqrt{\hat{u}\hat{v}}, \\ u + v = 2\sqrt{\hat{u}\hat{v}}, & \text{for } u > \sqrt{\hat{u}\hat{v}}. \end{cases}$$

Moreover, for any (u_+, v_+) on the curve $u + v = 2\sqrt{u_-v_-}$ for $u \ge \sqrt{u_-v_-}$, the solution of (0.1), (2.1) consists of a T-wave joining (u_-, v_-) with $(\sqrt{u_-v_-}, \sqrt{u_-v_-})$ and a 2-rarefaction wave joining $(\sqrt{u_-v_-}, \sqrt{u_-v_-})$ with (u_+, v_+).

Subcase 1.3. Consider now the case $(\hat{u}, \hat{v}) \in W_1(u_-, v_-)$ with $\hat{u} \ge \sqrt{u_-v_-}$. Again, it turns out that there is just one admissible second
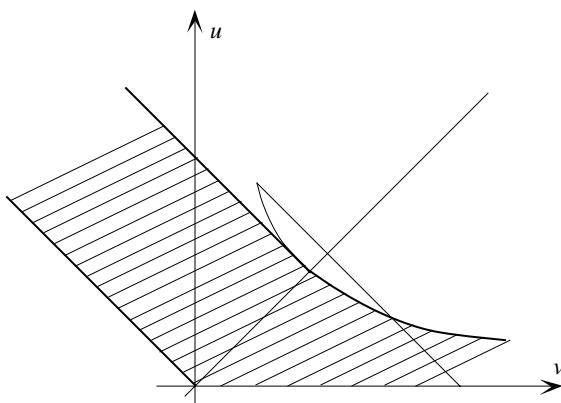

FIGURE 2.4.

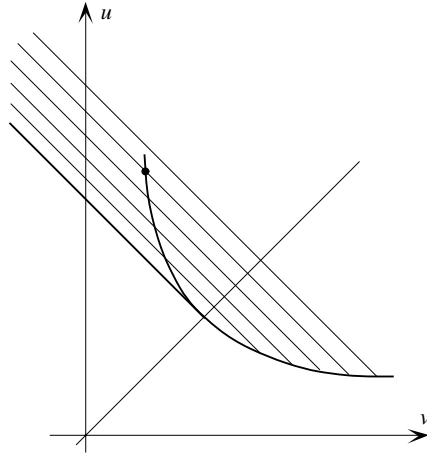FIGURE 2.5.

wave curve $W_2(\hat{u}, \hat{v})$, namely,

$$u + v = \hat{u} + \hat{v} \quad \text{for } u > \hat{v},$$

and it is clear that $\{W_2(\hat{u}, \hat{v})\}$ covers univalently the domain

$$\{u + v \geq 2\sqrt{u_- v_-}\} \cap \{u > v\} \cup \{0 < uv < u_- v_-\}$$

(see Figure 2.5) as $(\hat{u}, \hat{v})$ varies on $W_1(u_-, v_-)$ for $\hat{u} \geq \sqrt{u_- v_-}$.

Subcase 1.4. If $(\hat{u}, \hat{v}) \in W_1(u_-, v_-)$ with $\hat{u} < 0$, $W_2(\hat{u}, \hat{v})$ is the curve $uv = \hat{u}\hat{v}$, which covers univalently the domain $u < 0$, $v > 0$, as $\hat{u}$ varies from 0 to $-\infty$.

Subcase 1.5. Finally, if $(\hat{u}, \hat{v}) \in W_1(u_-, v_-)$ with $\hat{u} = 0$, any point $(0, \tilde{v})$ can be joined to $(\hat{u}, \hat{v})$ by a T-wave. For any $\tilde{v} > 0$ it is impossible to find another state which can be joined to $(0, \tilde{v})$ by a 2-rarefaction wave or a 2-shock wave; in other words, there is no second wave curve unless $u = 0$. However, for any $\tilde{v} \leq 0$, there exists a unique admissible T-wave $W_2(0, \tilde{v})$, namely $u + v = \tilde{v}$ for $v < 0$. Plainly, $\{W_2(0, \tilde{v})\}$ covers univalently the domain

$$\{u + v \leq 0, v \leq 0\} \text{ as } \tilde{v} \text{ varies from 0 to } -\infty$$
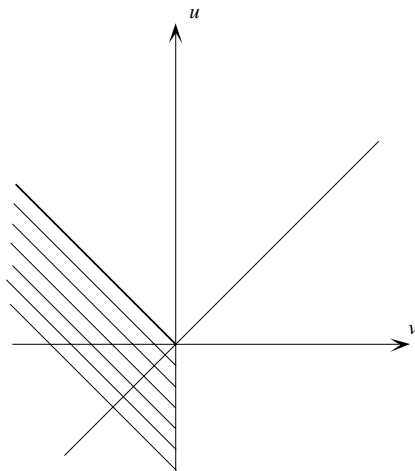
(see Figure 2.6).

FIGURE 2.6.

The above considered subcases 1.1–1.5 exhaust the discussion for the case when $0 < v_- < u_-$. Summarizing, we have shown that, for any state (u_+, u_+) in the (u, v)-plane, there exists a unique state $(\hat{u}, \hat{v})$ on the first wave curve $W_1(u_-, v_-)$ and a unique second wave curve $W_2(\hat{u}, \hat{v})$ which connects (u_+, v_+) to $(\hat{u}, \hat{v})$. Here, for any $(u_+, v_+) \in \{u + v \le 0, v \le 0, u \ge 0\}$ the second wave curve is defined by

$$\begin{cases} u = 0, & \text{for } u_+ + v_+ \le v \le u_- + v_- \\ u + v = u_+ + v_+, & \text{for } v \le u_+ + v_+. \end{cases}$$

Likewise, for any $(u_+, v_+) \in \{u \le 0, v \le 0\}$, the second wave curve is defined by

$$\begin{cases} u = 0, & \text{for } u_+ + v_+ \le v \le u_- + v_- \\ u + v = u_+ + v_+, & \text{for } u_+ \le u \le 0. \end{cases}$$

The discussion for the other cases of location of (u_-, v_-) is similar.

It is important to realize how the solution is built up in terms of the elementary wave types R_i, S_i, $i = 1, 2$, and T. This amounts to studying the *wave pattern* of any solution of the Riemann problem and amounts to analyzing the single cases in detail. The results are displayed in the forthcoming subsection.
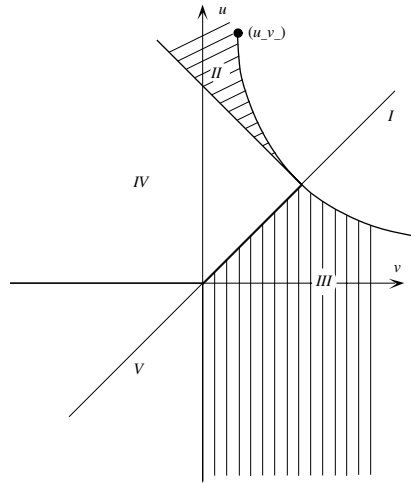
2b. *Riemann problem: Wave patterns of the solutions.*

FIGURE 2.7. The phase plane in Case 1.

Case 1. $0 < v_- < u_-$. Draw the curve $uv = u_-v_-$, which intersects with $u = v$ at $(\sqrt{u_-v_-}, \sqrt{u_-v_-})$; then draw the line $u + v = 2\sqrt{u_-v_-}$, $v < \sqrt{u_-v_-}$. These two curves, together with the coordinate axes, divide the (u, v)-plane into five domains I–V (cf. Figure 2.7). For any $(u_+, v_+) \in \mathrm{I}(u_-, v_-)$ there exists a unique state (u^*, v^*) on the curve $uv = u_-v_-$ (which is the intersection of the curves $u + v = u_+ + v_+$ and $uv = u_-v_-$) such that (u^*, v^*) can be joined to (u_-, v_-) on the right by a T-wave denoted by T, and (u_+, v_+) can be joined to (u^*, v^*) on the right by a 2-shock, denoted by S_2. In other words, the solution of the Riemann problem (0.1), (2.1) consists of a contact discontinuity and of a front shock wave. The wave pattern, $T - S_2$, is represented in Figure 2.8.1.

For any $(u_+, v_+) \in \mathrm{II}(u_-, v_-)$, there exists a unique state (u^*, v^*) on the curve $uv = u_-v_-$ which can be joined to (u_-, v_-) on the right by a T-wave denoted by T, and (u_+, v_+) can be joined to (u^*, v^*) on the right by a 2-rarefaction wave R_2. The wave pattern, $T - R_2$, is represented in Figure 2.8.2.

For any $(u_+, v_+) \in \mathrm{III}(u_-, v_-)$, there exists a unique state (u^*, v^*) on the curve $u + v = u_- + v_-$, with $u < v_-$, such that (u^*, v^*) can be joined to (u_-, v_-) on the right by a 1-shock S_1 and (u_+, v_+) can be

joined to (u^*, v^*) on the right by a T-wave. The resulting wave pattern is $S_1 - T$ (see Figure 2.8.3).

For any $(u_+, v_+) \in \mathrm{IV}(u_-, v_-)$ with $u_+ + v_+ > 0$, there exists a unique state $(\tilde{u}, \tilde{v})$, $\tilde{u} = \tilde{v} = (u_+ + v_+)/2$ and a unique state (u^*, v^*) (which is the intersection of the curves $uv = \tilde{u}\tilde{v}$ and $u + v = u_- + v_-$) such that (u^*, v^*) can be joined to (u_-, v_-) on the right by a 1-shock S_1, $(\tilde{u}, \tilde{v})$ can be joined to (u^*, v^*) on the right by a T-wave, followed by a 2-rarefaction wave up to (u_+, v_+). The resulting wave pattern is $S_1 - TR_2$ (see Figure 2.8.4.1).

For any $(u_+, v_+) \in \mathrm{IV}(u_-, v_-)$, with $u_+ + v_+ \leq 0$, there exists a unique state $(\tilde{u}, \tilde{v})$, $\tilde{u} = 0$ $\tilde{v} = u_+ + v_+$ and a unique state (u^*, v^*), $u^* = 0$, $v^* = u_- + v_-$ such that (u^*, v^*) can be joined to (u_-, v_-) on the right by a 1-shock, $(\tilde{u}, \tilde{v})$ can be joined to (u^*, v^*) on the right by a T-wave, and (u_+, v_+) can be joined to $(\tilde{u}, \tilde{v})$ on the right by a 2-rarefaction wave. The solution's wave pattern is $S_1 - T - R_2$, cf. Figure 2.8.4.2.

For any $(u_+, v_+) \in V(u_-, v_-)$, there exists a unique state $(\tilde{u}, \tilde{v})$, $\tilde{v} = u_+ + v_+$, $\tilde{u} = 0$ and a unique state (u^*, v^*), $u^* = 0$, $v^* = u_- + v_-$ such that (u^*, v^*) can be joined to (u_-, v_-) on the right by a 1-shock, $(\tilde{u}, \tilde{v})$ can be joined to (u^*, v^*) on the right by a T-wave, and (u_+, v_+) can be joined to $(\tilde{u}, \tilde{v})$ on the right by a 2-shock. This solution has wave pattern $S_1 - T - S_2$, cf. Figure 2.8.5.

Case 2. $v_- < u_- < 0$. As in Case 1, we divide the phase-plane into five domains I–V (Figure 2.9). The solution of the Riemann problem (0.1), (2.1) can be easily shown to have the same wave patterns as before (Figures 2.8).

Case 3. $v_- < 0 < u_-$. The two branches of the hyperbola $uv = u_- v_-$ divide the (u, v) plane into three regions, I–III (see Figure 2.10).

For any $(u_+, v_+) \in \mathrm{I}(u_-, v_-)$, the intersection point of $u + v = u_+ + v_+$ with $uv = u_- v_-$, $u > 0$, provides (u^*, v^*), which can be joined to (u_-, v_-) on the right by a T-wave, while (u_+, v_+) can be joined to (u^*, v^*) on the right by a 2-rarefaction wave. Thus, the solution's wave pattern is $T - R_2$, cf . Figure 2.11.1.

For any $(u_+, v_+) \in \mathrm{II}(u_-, v_-)$, the intersection point of $u + v = u_+ + v_+$, with $uv = u_- v_-$, $u > 0$, provides (u^*, v^*), which can be joined to (u_-, v_-) on the right by a T-wave, while (u_+, v_+) can be joined to (u^*, v^*) on the right by a 2-shock wave. Thus, the solution's wave pattern is $T - S_2$, cf. Figure 2.11.2.
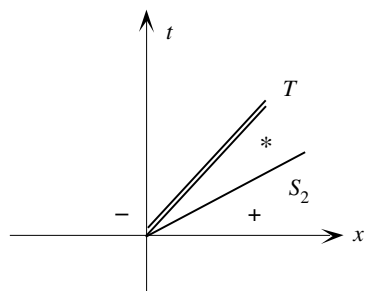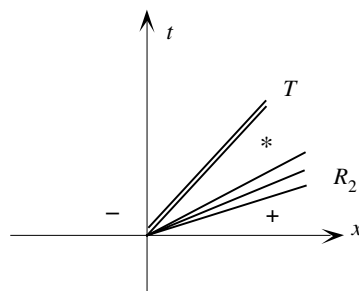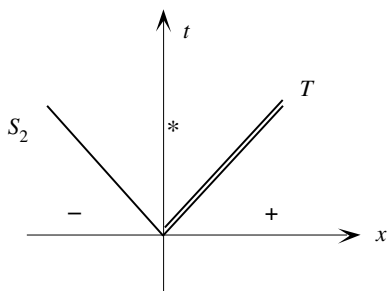
FIGURE 2.8.1
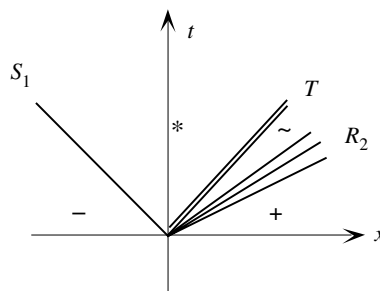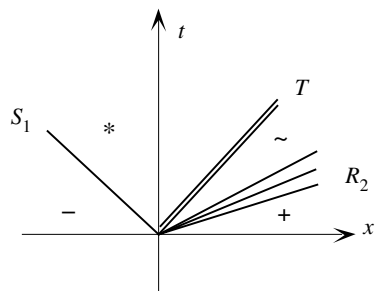
FIGURE 2.8.2

FIGURE 2.8.3
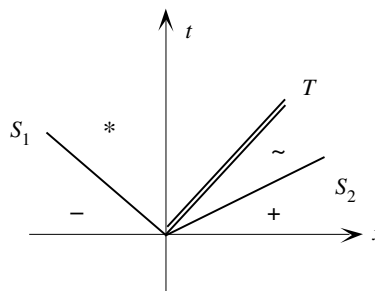
FIGURE 2.8.4.1

FIGURE 2.8.4.2

FIGURE 2.8.5

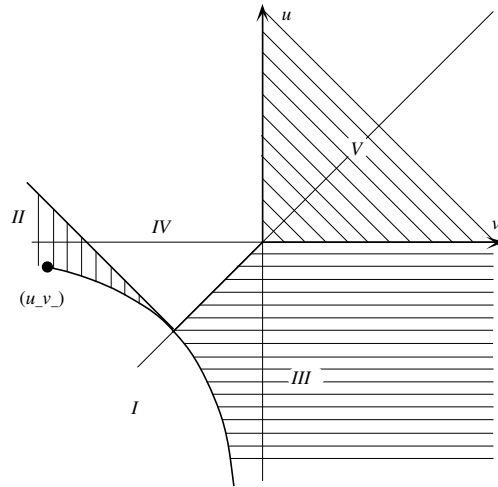FIGURES 2.8.1–2.8.5. Wave patterns in case 1.

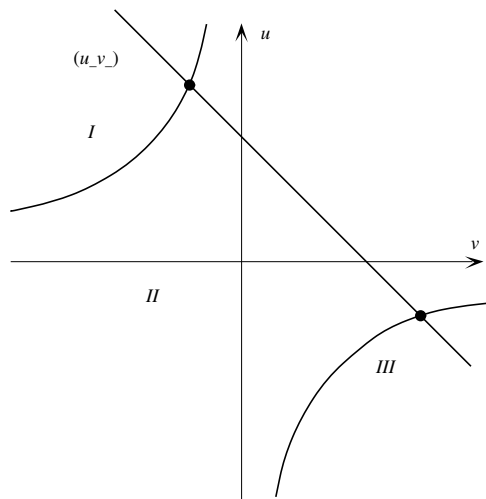FIGURE 2.9. The phase plane in Case 2.

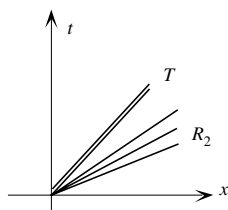FIGURE 2.10. The phase plane in Case 3.

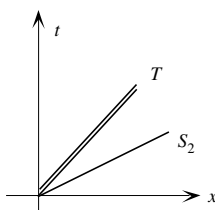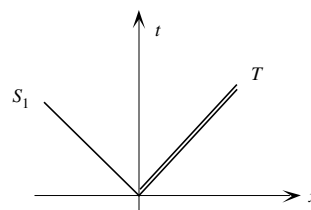FIGURE 2.11.1   FIGURE 2.11.2   FIGURE 2.11.3

FIGURES 2.11.1–2.11.3. Wave patterns in Case 3.

For any $(u_+, v_+) \in \text{III}(u_-, v_-)$, the intersection point of $u + v = u_- + v_-$, with $uv = u_+ v_+$, $u < 0$, provides (u^*, v^*), which can be joined to (u_-, v_-) on the right by a 1-shock, while (u_+, v_+) can be joined to (u^*, v^*) on the right by a T wave. The solution's wave pattern is $S_1 - T$, cf. Figure 2.11.3.

Case 4. $0 < u_- < v_-$. Draw the curve $uv = u_- v_-$, which intersects with $u = v$ at $(\sqrt{u_- v_-}, \sqrt{u_- v_-})$; then draw the line $u + v = 2\sqrt{u_- v_-}$, $u > \sqrt{u_- v_-}$. After tracing the line $u + v = u_- + v_-$, which intersects with $u = v$ at $((u_- + v_-)/2, (u_- + v_-)/2)$, draw the curve $uv = ((u_- + v_-)/2)^2$. These curves, together with the coordinate axes divide the (u, v)-plane into six domains I–VI (see Figure 2.12).

For any $(u_+, v_+) \in \text{I}(u_-, v_-)$, there exists a unique state $(\tilde{u}, \tilde{v})$ on the curve $uv = ((u_- + v_-)/2)^2$, which is the intersection of the curves $uv = ((u_- + v_-)/2)^2$ and $u + v = u_+ + v_+$, with $u > u_+$, such that $(u^*, v^*) = ((u_- + v_-)/2, (u_- + v_-)/2)$ can be joined to (u_-, v_-) on the right by a 1-rarefaction wave and $(\tilde{u}, \tilde{v})$ can be joined to (u^*, v^*) on the right by a T-wave. At last, (u_+, v_+) can be joined to $(\tilde{u}, \tilde{v})$ on the right by a 2-shock. The resulting solution has wave pattern $R_1 - T - S_2$ or $R_1 T - S_2$, see Figure 2.13.1.

For any $(u_+, v_+) \in \text{II}(u_-, v_-)$, there exists a unique state (u^*, v^*) such that (u^*, v^*) can be joined to (u_-, v_-) on the right by a 1-rarefaction wave and (u_+, v_+) can be joined to (u^*, v^*) on the right by a T-wave. The solution has wave pattern $R_1 - T$, as depicted in Figure 2.13.2.
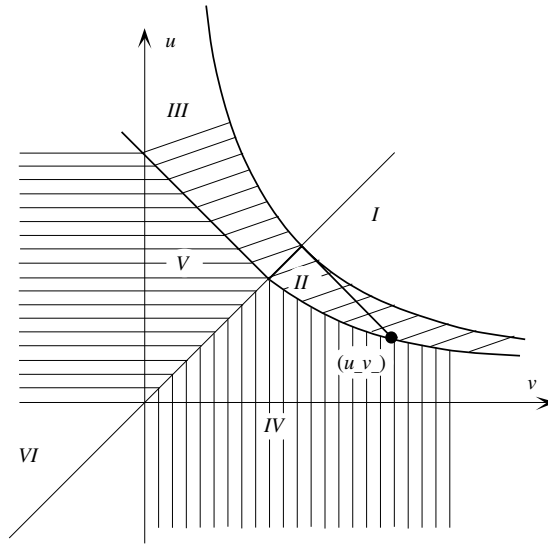
FIGURE 2.12. The phase plane in Case 4.

For any $(u_+, v_+) \in \mathrm{III}(u_-, v_-)$, there are two subcases, according to whether $u + v = u_+ + v_+$ intersects first the line $u = v$ or the curve $uv = ((u_- + v_-)/2)^2$, $u > (u_- + v_-)/2$. Denoting, by $(\tilde{u}, \tilde{v})$, the above intersection in both the two subcases, in the former case we find that the intersection point (u^*, v^*) of $uv = \tilde{u}\tilde{v}$ with $u + v = u_- + v_-$ can be joined to (u_-, v_-) on the right by a 1-rarefaction wave, and $(\tilde{u}, \tilde{v})$ can be joined to (u^*, v^*) on the right by a T-wave followed by a 2-rarefaction wave up to (u_+, v_+). The solution's pattern is, therefore, $R_1 - TR_2$. In the latter case, the state $(u^*, v^*) = ((u_- + v_-)/2, (u_- + v_-)/2)$ can be joined to (u_-, v_-) on the right by a 1-rarefaction wave, accompanied by a T-wave up to $(\tilde{u}, \tilde{v})$. At last, (u_+, v_+) can be joined to $(\tilde{u}, \tilde{v})$ on the right by a 2-rarefaction wave. The solution's pattern is, therefore, $R_1 T - R_2$. The wave patterns in both subcases are depicted in Figure 2.13.3.

For any $(u_+, v_+) \in \mathrm{IV}(u_-, v_-)$, the unique intersection point (u^*, v^*) of the curves $u + v = u_- + v_-$ and $uv = u_+ v_+$ can be joined to (u_-, v_-) on the right by a 1-shock wave, and (u_+, v_+) can be joined to (u^*, v^*) on the right by a T-wave. The solution's pattern, $S_1 - T$, is depicted in Figure 2.13.4.
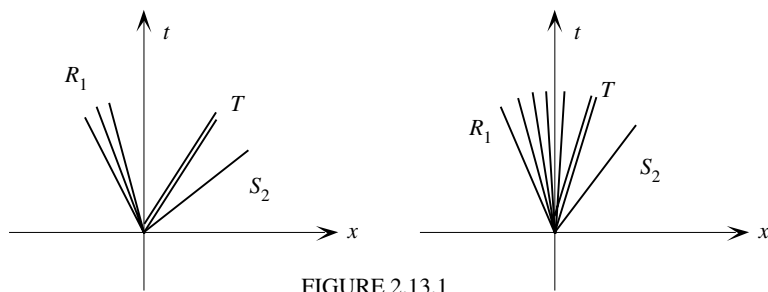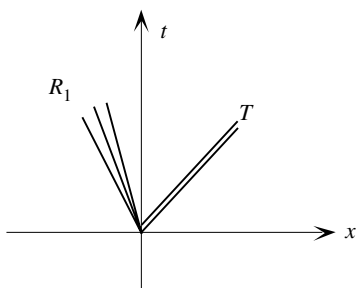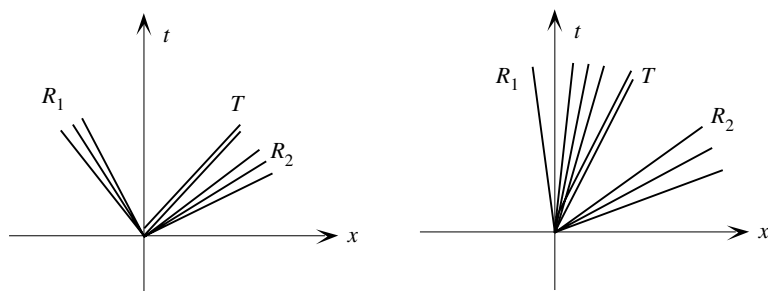
FIGURE 2.13.1

FIGURE 2.13.2

FIGURE 2.13.3

FIGURES 2.13.1–2.13.3. Wave patterns in Case 4.

For any $(u_+, v_+) \in \mathrm{V}(u_-, v_-)$, there are two subcases according to whether $u + v = u_+ + v_+$ intersects first the line $u = v$ or the line $u = 0$. Denoting by $(\tilde{u}, \tilde{v})$ the above intersection point in both the two subcases, in the former case we find that the intersection point (u^*, v^*) of $uv = \tilde{u}\tilde{v}$, with $u + v = u_- + v_-$, can be joined to (u_-, v_-) on the right by a 1-shock wave and $(\tilde{u}, \tilde{v})$ can be joined to (u^*, v^*) on the right by a T-wave, followed by a 2-rarefaction wave up to (u_+, v_+). The wave pattern is then $S_1 - T R_2$. In the latter case, the state $(0, v^*)$, which is the intersection of $u + v = u_- + v_-$ with $u = 0$ can be joined to (u_-, v_-) on the right by a 1-shock wave, whereas $(\tilde{u}, \tilde{v}) = (0, \tilde{v})$ can be joined to $(0, v^*)$ on the right by a T-wave. At last, (u_+, v_+) can be joined to $(0, \tilde{v})$ on the right by a 2-rarefaction wave. The solution's wave pattern is, therefore, $S_1 - T - R_2$. The wave patterns in both subcases are depicted in Figure 2.13.5.

For any $(u_+, v_+) \in \mathrm{VI}(u_-, v_-)$, there is a unique intersection point (u^*, v^*) of the lines $u + v = u_- + v_-$ and $u = 0$, and there is a unique intersection $(\tilde{u}, \tilde{v})$ point of the lines $u + v = u_+ + v_+$ and $u = 0$: (u^*, v^*) can be joined to (u_-, v_-) on the right by a 1-shock and can be joined to (u^*, v^*) on the right by a T-wave. At last, (u_+, v_+) can be joined to $(\tilde{u}, \tilde{v})$ on the right by a 2-shock wave. The solution's pattern is $S_1 - T - S_2$ and is depicted in Figure 2.13.6.

Case 5. $u_- < v_- < 0$. As in case 4, we divide the phase plane into six domains (see Figure 2.14). The solution of the Riemann problem has the same wave patterns as in Case 4.

Case 6. $u_- < 0 < v_-$. Draw the curve $uv = u_- v_-$ and the line $u + v = u_- + v_-$, which intersects with $u = v$ at $((u_- + v_-)/2, (u_- + v_-)/2)$; then draw the curve $uv = ((u_- + v_-)/2)^2$. These curves, together with the coordinate axes, divide the (u, v)-plane into five domains I, II, III$_1$, III$_2$, IV (see Figure 2.15).

For any $(u_+, v_+) \in \mathrm{I}(u_-, v_-)$, there is a unique intersection point (u^*, v^*) of the curves $u + v = u_- + v_-$ and $uv = u_+ v_+$; it can be joined to (u_-, v_-) on the right by a 1-shock, whereas (u_+, v_+) can be joined to (u^*, v^*) on the right by a T-wave. The solution's pattern, $S_1 - T$, is displayed in Figure 2.16.1.

For any $(u_+, v_+) \in \mathrm{II}(u_-, v_-)$, there is a unique intersection point (u^*, v^*) of the curves $u + v = u_- + v_-$ and $uv = u_+ v_+$; it can be joined to (u_-, v_-) on the right by a 1-rarefaction wave, whereas (u_+, v_+) can
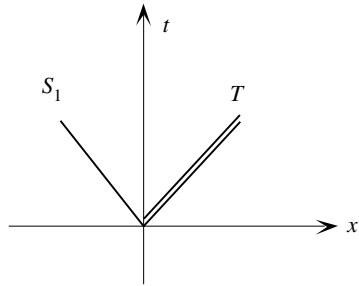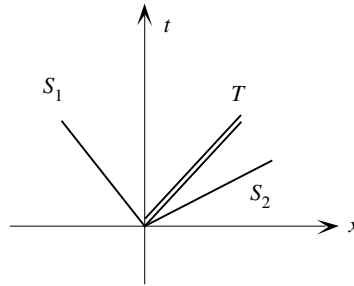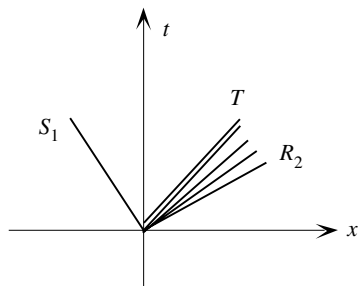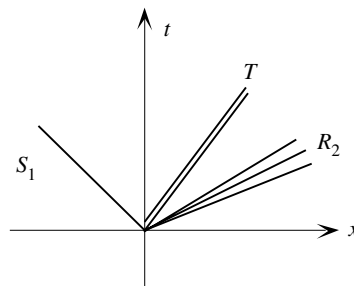
FIGURE 2.13.4

FIGURE 2.13.6

FIGURE 2.13.5.1

FIGURE 2.13.5.2

FIGURES 2.13.4–2.13.6. More wave patterns for Case 4.

be joined to (u^*, v^*) on the right by a T-wave. The solution's pattern, denoted by $R_1 - T$, is shown in Figure 2.16.2.

For any $(u_+, v_+) \in \mathrm{III}_1(u_-, v_-)$, denote, by (u^*, v^*), the unique intersection point of the curves $u + v = u_- + v_-$ and $u = v$, that is, $u^* = v^* = v = (u_- + v_-)/2$. (u^*, v^*) can be joined to (u_-, v_-) on the right by a 1-rarefaction wave. Denote by $(\tilde{u}, \tilde{v})$ the unique intersection point of the curves $uv = (u_- + v_-)^2/4$ and $u + v = u_+ + v_+$: $(\tilde{u}, \tilde{v})$ can be joined on the right to (u^*, v^*) by a T-wave, whereas (u_+, v_+) can be joined to $(\tilde{u}, \tilde{v})$ on the right by a 2-shock wave. The solution has wave pattern $R_1 T - S_2$, as shown in Figure 2.16.3.1.
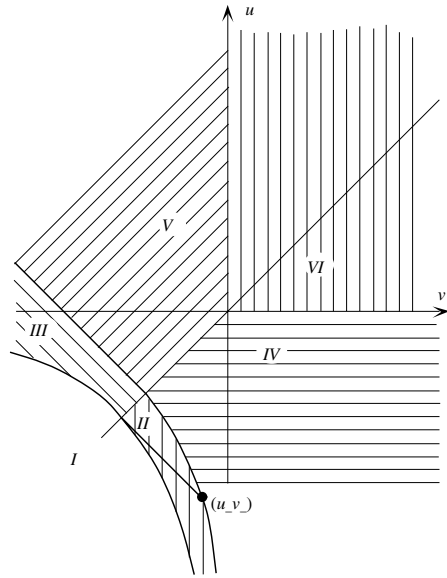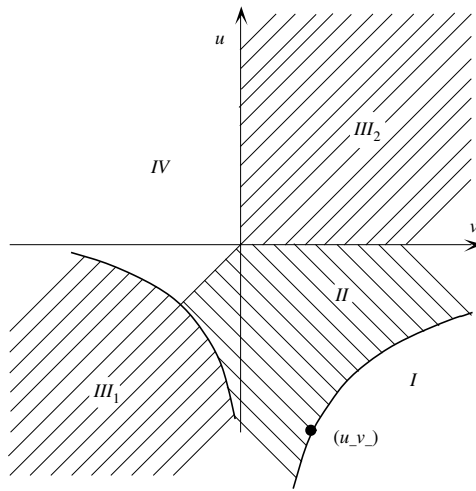
FIGURE 2.14. The phase plane in Case 5.

FIGURE 2.15. The phase plane in Case 6.

For any $(u_+, v_+) \in \text{III}_2(u_-, v_-)$, the unique intersection point $(u^*, 0)$ of the lines $u + v = u_- + v_-$ and $v = 0$ (that is, $u^* = u_- + v_-$) can be joined to (u_-, v_-) on the right by a 1-rarefaction wave. On the other hand, the unique intersection point $(\tilde{u}, 0)$ of the lines $u + v = u_+ + v_+$ and $v = 0$ (that is, $\tilde{u} = u_+ + v_+$) can be joined to (u^*, v^*) on the right by a T-wave, while (u_+, v_+) can be joined to $(\tilde{u}, 0)$ on the right by a 2-shock wave. The solution has wave pattern $R_1 - T - S_2$, as shown in Figure 2.16.3.2.

For any $(u_+, v_+) \in \text{IV}(u_-, v_-)$, there are three subcases according to whether the line $u_+ + v_+$ meets first (i) the curve $uv = ((u_- + v_-)/2)^2/4$ for $u > (u_- + v_-)/2$; (ii) the line $u = v$; or (iii) the axis $v = 0$. In the first subcase, the solution has pattern $R_1 T - R_2$, in the second subcase, $R_1 - T R_2$, and in the third case it has pattern $R_1 - T - R_2$ (see Figure 2.16.4). Indeed, this can be easily checked if one proceeds as above, upon taking: in case (i), $(u^*, v^*) = ((u_- + v_-)/2, (u_- + v_-)/2)$, and $(\tilde{u}, \tilde{v})$ as the intersection of $u + v = u_+ + v_+$ with $uv = (u_- + v_-)^2/4$; in case (ii), $(\tilde{u}, \tilde{v})$ as the intersection point of $u + v = u_+ + v_+$ with $u = v$, and (u^*, v^*) as the intersection point of $u + v = u_- + v_-$ with $uv = ((u_- + v_-)/2)^2$, in case (iii), (u^*, v^*) as the intersection point of $u + v = u_- + v_-$, with $v = 0$, and $(\tilde{u}, \tilde{v})$ as the intersection point of $u + v = u_+ + v_+$, with $v = 0$.

The results of the above subsections can be synthesized as follows.

Theorem 2.1. *For any given data (u_-, v_-), (u_+, v_+) on the (u, v) plane, there exists a unique admissible solution of the Riemann problem (0.1), (2.1). This solution consists of at most four states and three waves. The wave pattern of the solution is one of the following:*

$T - S_2 \qquad (\text{or } S_2) \qquad R_1 - T \qquad (\text{or } R_1)$

$T - R_2 \qquad (\text{or } R_2) \qquad R_1 - T - S_2 \ (\text{or } R_1 T - S_2)$

$S_1 - T \qquad (\text{or } S_1) \qquad R_1 - T - R_2 \ (\text{or } R_1 T - R_2 \text{ or } R_1 - T R_2)$

$S_1 - T - S_2$

$S_1 - T - R_2 \ (\text{or } S_1 - T R_2)$

If we introduce now the *Riemann invariants* by

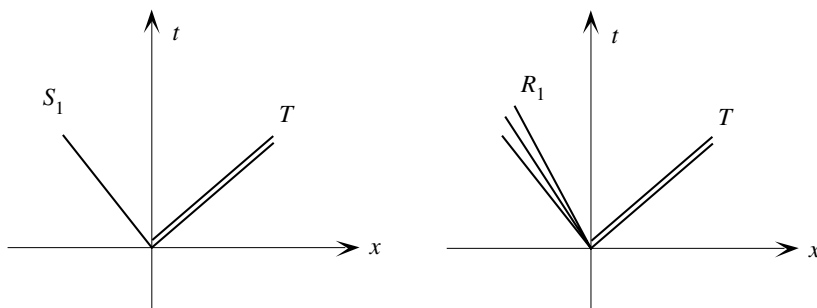$$(2.2) \qquad \begin{aligned} r &= u + v, \\ s &= uv. \end{aligned}$$

FIGURE 2.16.1–2
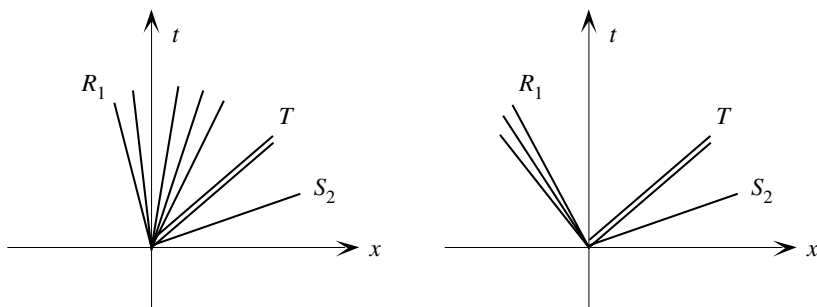
FIGURE 2.16.3–4

FIGURE 2.16. Wave patterns for Case 6.

This defines a map $\Phi : (u, v) \in \mathbf{R}^2 \longrightarrow (r, s) \in \{r^2 - 4s \geq 0\}$. By the very structure of the solution, one can prove

Theorem 2.2. *For any given data* (r_-, s_-), $(r_+, s_+) \in \{r^2 - 4s \geq 0\}$, *the unique admissible solution of* (0.1), (2.1) *is still contained in* $\{r^2 - 4s \geq 0\}$, *and it satisfies*

$$\min\{r_\pm\} \leq r(x, t) \leq \max\{r_\pm\}$$
(2.3) $$\min\{0, s_\pm\} \leq s(x, t) \leq \max\{s_\pm, (\min |r_\pm|)^2/4\}.$$

3. General initial value problem. Consider the initial value problem

(3.1)
$$\begin{cases} u_t + (u(1-v))_x = 0 \\ \\ v_t + (v(1+u))_x = 0 \\ (u(x,0), v(x,0)) = (u_0, v_0), \quad x \in \mathbf{R}, \end{cases} \quad \text{in } \mathbf{R} \times \mathbf{R}^+,$$

where u_0, v_0 are bounded measurable functions such that the associated r and s, (cf. (2.2)), denoted by r_0, s_0, are of bounded variation. (Of course, this is true if u_0, v_0 themselves are of bounded variation.) Define

(3.2)
$$\underline{r} := \min\{r_0(x), x \in \mathbf{R}\}, \quad \tilde{r} := \max\{r_0(x), x \in \mathbf{R}\}$$
$$\underline{s} := \min\{s_0(x), x \in \mathbf{R}\}$$

$$D := \{\min\{0, \underline{s}\} \le s \le r^2/4; \underline{r} \le r \le \tilde{r}\}.$$

In the following, we shall say that a solution (u, v) belongs to D if the associated Riemann invariants r, s belong to D. Using the results of the previous section, it can be easily shown that the following holds.

Lemma 3.1. *Any solution of the Riemann problem* (3.1) *with data* $(u_\pm, v_\pm)$ *belonging to D still belongs to D.*

To prove an existence theorem for (3.2), relying on Glimm's ideas [**3**], we shall use Glimm's algorithm in a slightly modified context. Let us fix a space mesh size $h > 0$ and determine the corresponding time mesh size s by $s = \Lambda^{-1}h$, where Λ is a fixed upper bound for the supremum over D of the absolute values of the characteristic speeds $\lambda_i(u, v)$, $i = 1, 2$, so that waves emanating simultaneously from points separated by a distance $2h$ will not interact on a time interval of length s.

Let us partition the upper half-plane of the (x, t)-plane into strips

$$S_n := \{(x, t); -\infty < x < \infty; ns \le t < (n+1)s\},$$

$n = 0, 1, 2, \ldots$, and focus on the mesh points $[kh, ns]$ with $k + n$ even. Assuming that the approximate solution $(u_h(x, t), v_h(x, t))$ has been

determined in

$$\bigcup_{k=0}^{n-1} S_k,$$

we shall describe how to construct the solution in the strip S_n. For every m with $m + n$ odd, consider the random mesh point $[y_{m,n}, ns]$, where $y_{m,n} = (m + a_{m,n})h$, $a_{m,n} \in \mathfrak{U} = \Pi_{m,n}[-1, 1]$, the measure space which is the product of copies of the interval $[-1, 1]$ equipped with the normalized Lebesgue measure, one copy for each rectangle of base $2h$ and height s, having the point (mh, ns) at the top center of the rectangle, and then define

$$u_{m,n} = u_h(y_{m,n}, ns^-), \qquad v_{m,n} = v_h(y_{m,n}, ns^-).$$

To initiate the algorithm, at $n = 0$, we set

$$u_h(x, 0^-) = u_0(x), v_h(x, 0^-) := v_0(x), \qquad x \in \mathbf{R}.$$

Consider now any mesh point $[kh, ns]$ with $k + n$ even. Let $(u_h(x, t), v_h(x, t))$ denote the restriction to $\{(x, t) : (k - 1)h \leq x < (k + 1)h; ns \leq t < (n + 1)s\}$ of the solution of the Riemann problem consisting of the equations (0.1) supplemented with data

$$(3.3) \qquad (u_h(x, ns), v_h(x, ns)) = \begin{cases} (u_{k-1,n}, v_{k-1,n}), & x < kh \\ (u_{k+1,n}, v_{k+1,n}), & x > kh. \end{cases}$$

The solvability of this problem relies upon Theorem 2.1. The above procedure determines $(u_h(x, t), v_h(x, t))$ in the strip S_n. Since, by virtue of Lemma 3.1, the approximate solution $(u_h(x, t), v_h(x, t))$ still remains in the domain D, this approximate solution can be indeed defined for all $t > 0$. According to the classical Glimm method (cf. [**3,2**]), in order to show the convergence and the consistency of the algorithm we should prove the uniform boundedness of the approximate solution and of its total variation in x. The solution's uniform boundedness can be read off from Lemma 3.1. Concerning the uniform boundedness of the total variation, some difficulties arise, since, as it will be shown below (Lemmas 3.2, Example 3.5), uniform boundedness of the total variation can be proved for the quantities r and s, but in general *not* for u and v themselves. Thus, the classical
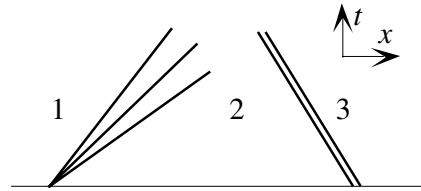
FIGURE 3.1. Interaction $R_2 + T$.

Glimm method is not applicable to the present situation. However, the adaptation of the method provided by [**14**] will enable us to overcome this difficulty (see Theorem 3.3 below).

Let us define as *strength* of a wave the associated change in r for any T-wave and the change in s for either shock or rarefaction waves. We shall denote such strength by $|T|$, respectively, $|S|$, $|R|$. To prove the uniform boundedness of the total variation of r and s, we need to investigate all possible wave interactions and to show that the overall wave strength after the interaction does not exceed that before the interaction.

I. *Interaction of a 2-rarefaction wave with a T-wave.* $R_2 + T$ (see Figure (3.1)). Denote the states joined by R_2 by (1) and (2), those joined by T by (2) and (3). Now let us solve the Riemann problem determined by (1) as left state and (3) as right state; new waves will arise (which we shall denote by primed letters) which determine the wave pattern of the solution resulting from the interaction (*outgoing wave pattern*). Indeed, various possibilities arise, depending on the relative location of the states (1), (2) and (3).

Case 1. Let (1) and (2) belong to the same domain $\{v > 0, u > v\}$ (or $\{u < 0, u > v\}$). According to the location of (3), we have three cases:

1(a)   For any state (3) located above the state A, which is the intersection of the curves $uv = u_2v_2$ and $u + v = 2\sqrt{u_1v_1}$, the outgoing wave pattern is $T' - R_2'$, the intermediate state (4) being characterized as the intersection of $uv = u_1v_1$ with $u + v = u_3 + v_3$ (see Figure 3.2.a).

1(b)   For any state (3) located below the state B, which is the intersection of the curves $uv = u_2v_2$ and $u = v$, the wave pattern
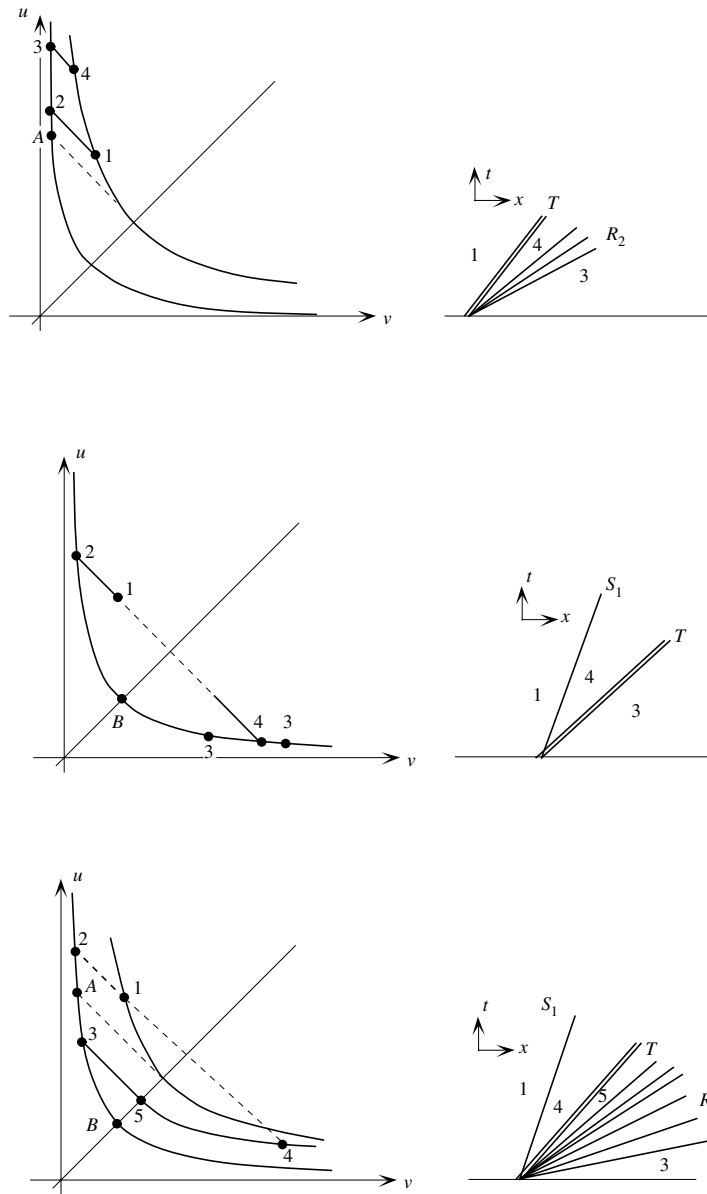
FIGURE 3.2.a–c. Outgoing waves for the $R_2 + T$ interaction: first case.

is $S_1' - T'$, the intermediate state (4) being characterized by $u = v_2$, $v = u_2$ (see Figure 3.2.b).

1(c) For any state (3) located between the states A and B defined above, the outgoing wave pattern is $S_1' - T'R_2'$, the intermediate states (4), (5) being characterized as follows: (5) as the intersection of $u = v$ with $u + v = u_3 + v_3$, (4) as the intersection of $uv = u_5v_5$ with $u + v = u_1 + v_1$ (see Figure 3.2.c).

Plainly, $|R_2'| = |R_2|$, $|T'| = |T|$ in case 1(a), $|S_1'| = |R_2|$, $|T'| = |T|$ in case 1(b), $|S_1'| + |R_2'| = |R_2|$, $|T'| = |T|$ in case 1(c). *Case* 2. Let (1) belong to $\{v > 0, u > v\}$ and (2) belong to $\{u > 0, v < 0\}$ (or (1) $\in \{u < 0, u > v\}$ and (2) $\in \{u > 0, v < 0\}$).

Here two kinds of wave patterns arise, corresponding to different locations of the state (3):

2(a) For any state (3) located above A, A being defined as in 1(a) above, the outgoing wave pattern is $T' - R_2'$. Here the intermediate state (4) is as in 1(a) above (see Figure 3.3.a).

2(b) For any state (3) located between A and B, where B is the intersection of the curves $uv = u_2v_2$ and $u + v = 0$, and A is as above, the outgoing wave pattern is $S' - T' - R_2'$; the intermediate states (4) and (5) are as in 1(c) above (cf. Figure (3.3.b)). The same outgoing wave pattern arises if (3) is located below the state (B) defined as in 1(b). In this case, the intermediate states (4), (5) are characterized by $u_0 = 0$, $v = u_1 + v_1$, and $u_5 = 0$, $v_5 = u_3 + v_3$ (see Figures 3.3.b, 3.3.c).

It is easy to show that $|R_2'| = |R_2|$ and $|T'| = |T|$ in Case 2.a, and $|S_1'| + |R_2'| = |R_2|$ and $|T'| = |T|$, both cases in 2(b).

Case 3. Both states (1) and (2) belong to $\{u > 0, v < 0\}$. Here there is just one kind of outgoing wave pattern, namely $T' - R_2'$. The intermediate state (4) is the intersection of $u + v = u_3 + v_3$ and $uv = u_1v_1$. Plainly, $|T'| = |T|$ and $|R_2'| = |R_2|$ (see Figure 3.4).

II. *Interaction of a* 2-*shock with a* T-*wave.* (See Figure 3.5.) Deriving the outgoing wave pattern amounts to solving the Riemann problem for the states (1) and (3). To do this, we have to understand in which relative locations the states do occur. Since (1) is joined to (2) on the right by a 2-shock S_2, this can only happen if $u_1 > v_1$ and if (2) is located on the line $u + v = u_1 + v_1$ with $v_1 < u_2 < u_1$. It turns out that, no matter where the states (2) and (3) are located, the outgoing
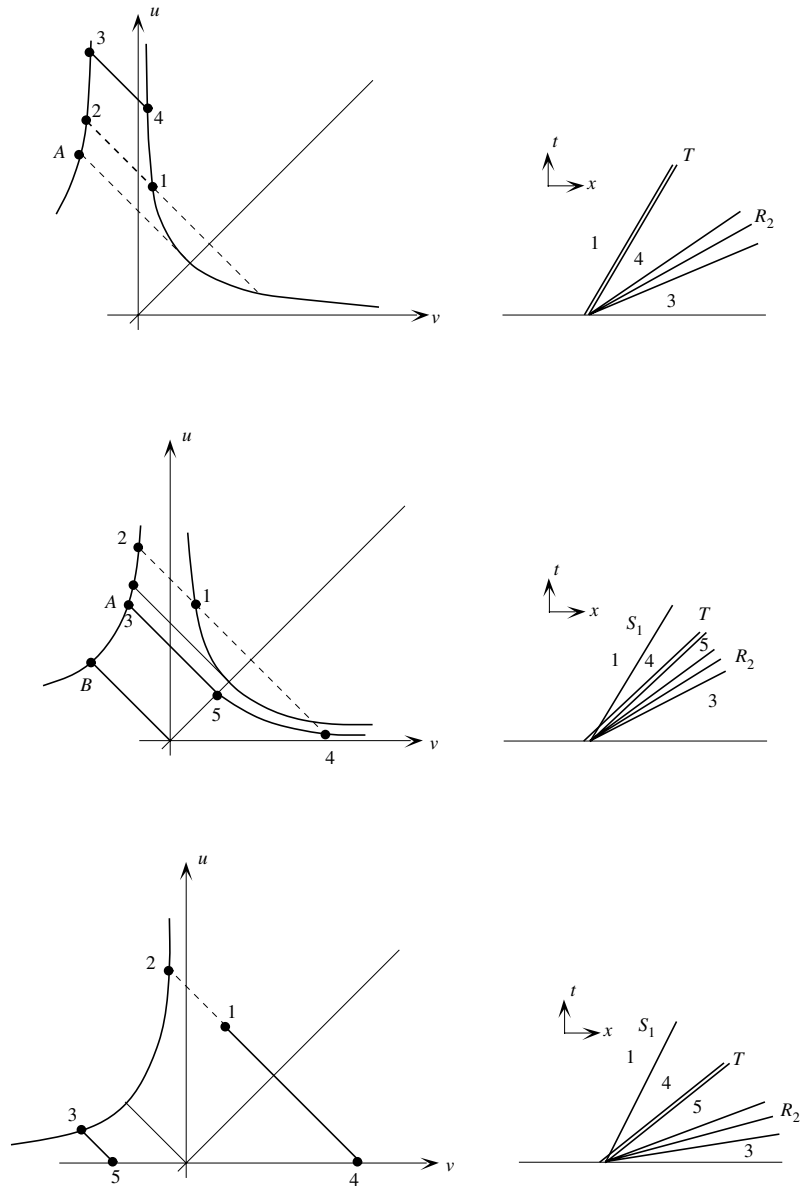
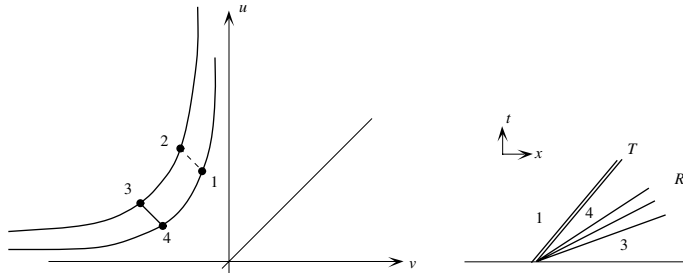FIGURE 3.3.a–c. Outgoing waves for the $R_2 + T$ interaction: second case.

FIGURE 3.4. Outgoing waves for the $R_2 + T$ interaction: third case.

wave pattern is the same, namely $T' - S_2'$, and $|T'| = |T|$, $|S_2'| = |S_2|$ (see Figure 3.6).

III. *Interaction of a 2-rarefaction wave with a 2-shock wave.* (See Figure 3.7.) Of course, the relative locations of states (1) and (2) are the same as those discussed *sub* item I, so we may refer again to Figures
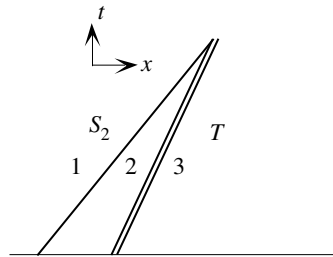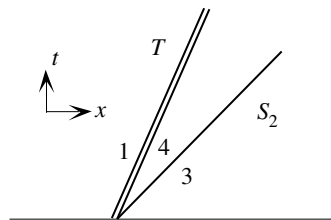

FIGURE 3.5. Interaction $S_2 + T$.

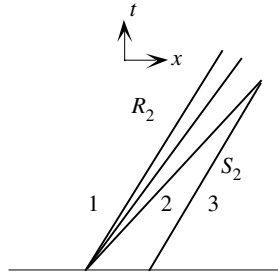FIGURE 3.6. Outgoing waves for the $S_2 + T$ interaction.

FIGURE 3.7. Interaction $R_2 + S_2$.

3.2, 3.3, 3.4. Various cases occur, as indicated below.

Case 1. Both (1) and (2) lie in the domain $\{v > 0, u > v\}$ (or $\{u < 0, u > v\}$). There are three kinds of outgoing wave patterns corresponding to the relative location of states (1), (2) and (3), the latter state lying on the line $u + v = u_2 + v_2$ with $v_2 < v_3 < v_B = u_2$ because (3) is joined to (2) on the right by a 2-shock (cf. Figure (3.8)); indeed, (1) can be joined to (3) by a single wave, namely either R_2', or S_2', or else S_1'. In fact, R_2' occurs whenever (3) is located between (1) and (2), and $|R_2'| < |R_2|$ holds; S_2' occurs if (3) lies between (1) and $A \equiv (v_1, u_1)$ (in this case $|S_2'| < |S_2|$ holds); while S_1' occurs if (3) lies between A and $B \equiv (v_2, u_2)$, in which case $|S_1'| < |R_2|$ holds (see Figures 3.9.a–c).

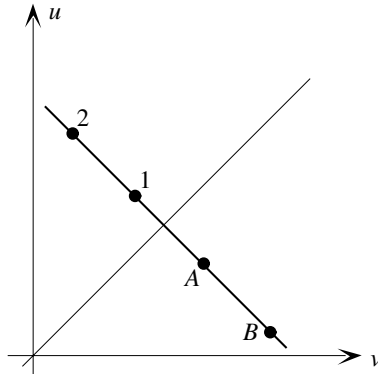*Case* 2. (1) $\in \{v > 0, u > v\}$ and (2) $\in \{u > 0, v < 0\}$ (or (1)

FIGURE 3.8. Location of states (1) and (2).

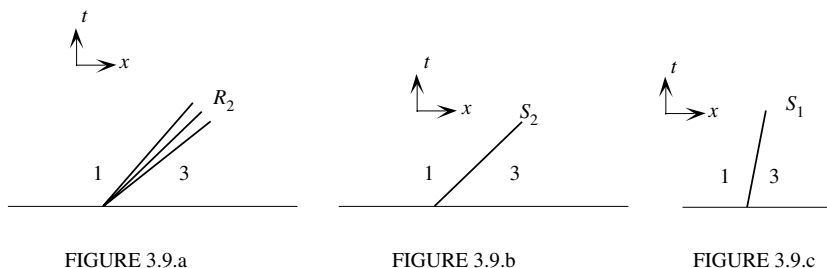FIGURE 3.9.a   FIGURE 3.9.b   FIGURE 3.9.c

FIGURE 3.9. Outgoing waves for the $R_2 + S_2$ interaction.

$\in \{u < 0, u > v\}$ and (2) $\in \{u > 0, v < 0\}$). This case is similar to Case 1 above: there are three kinds of outgoing waves, R_2', S_2', S_1', satisfying, respectively, $|R_2'| < |R_2|$, $|S_2'| < |S_2|$, $|S_1'| < |R_2|$.

Case 3. Both (1) and (2) lie in $\{u > 0, v < 0\}$. This case as well gives rise to the same outgoing waves as in Case 1 above.

IV. *Interaction of a 2-shock with a 2-rarefaction wave*: $S_2 + R_2$. (See Figure 3.10.)

For this interaction, from the fact that—as in item II above—(1) is joined to (2) on the right by a 2-shock S_2, we infer that $u_1 > v_1$ and (2) is located on the line $u + v = u_1 + v_1$ with $v_1 < u_2 < u_1$. On the other hand, since (2) is joined to (3) on the right by a 2-rarefaction wave, a further restriction holds, namely $u_2 > v_2$. As a consequence, we easily deduce that the outgoing wave pattern consists of a single wave, namely either S_2' or R_2', with $|S_2'| < |S_2|$, $|R_2'| < |R_2|$, respectively (see Figure 3.11).
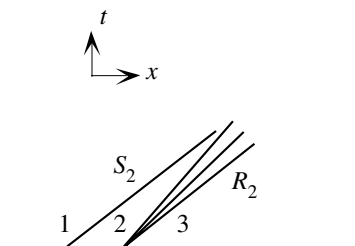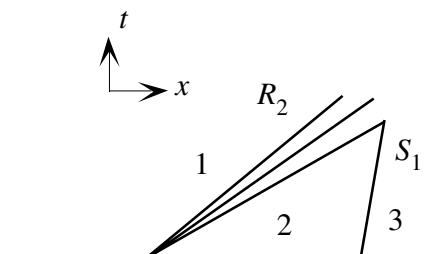

FIGURE 3.10. The interaction $S_2 + R_2$.

FIGURE 3.11. Outgoing waves for the $S_2 + R_2$ interaction.

V. *Interaction of a 2-rarefaction wave with a 1-shock:* $R_2 + S_1$. (See Figure 3.12.)

VI. *Interaction of a 2-shock with a 1-rarefaction wave.* $S_2 + R_1$. (See Figure 3.14.)

By considering the relative location of states (1), (2), (3), it follows that there is just one outgoing wave pattern, consisting of a single wave S_1', with $|S_1'| = |R_2| + |S_1|$. In fact, (3) must be located on $u + v = u_1 + v_1 = u_2 + v_2$ with $v_3 > v_B = u_2$, as shown in Figure 3.13 since (3), as right-hand state, is joined to (2) by a 1-shock.

As in items II and IV above, (1) is joined to (2) on the right by a 2-shock S_2, so $u_1 > v_1$ and (2) is located on the line $u + v = u_1 + v_1$ with $v_1 < u_2 < u_1$. On the other hand, (2) is joined to (3) on the right by a
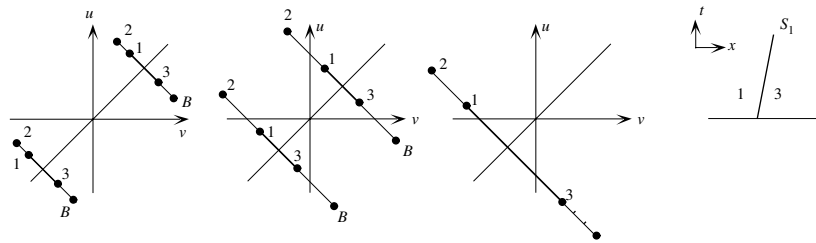

FIGURE 3.12. The interaction $R_2 + S_1$.

FIGURE 3.13. States' location and outgoing wave for $R_2 + S_1$.

1-rarefaction wave; thus (2) is restricted by $u_2 < v_2$ and (3) is located on $u + v = u_1 + v_1 = u_2 + v_2$, with $u_3 > u_2$, $u_3 < v_3$. Therefore, there is only one kind of outgoing wave pattern, consisting of a single wave, S_2', with $|S_2'| = |S_2| + |R_1|$.

The remaining wave interactions can be treated similarly. Summing up the results of the previous analysis, and recalling Lemma 3.1, we conclude

Lemma 3.2. *In any possible interaction, if the incoming waves are contained in the domain D, then the outgoing waves do the same, and the summation of the wave strength of the outgoing waves does not exceed that of the incoming waves.*

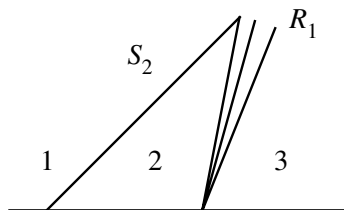In view of the structure of the algorithm outlined above, it is obvious

FIGURE 3.14. The interaction $S_2 + R_1$.

that Lemma 3.2 provides the uniform boundedness of the total variation (in x) of the approximate solution in terms of the variables r, s. As a consequence, the modification of Glimm's compactness argument provided by [**14**] permits one to conclude

Theorem 3.3. *Let $a \in \mathfrak{U}$ and $(u_0(x), v_0(x))$ be any initial datum of bounded variation in r, s. Then, for any sequence $\{h\}$ of mesh lengths which approaches zero, there is a subsequence $\{h_n\}$ and a function (u, v) such that, for any $T > 0$, $(u_{h_n a}(\cdot, t), v_{h_n a}(\cdot, t))$ converges in L^1_{loc} to $(u(\cdot, t), v(\cdot, t))$ uniformly, for $0 \le t \le T$.*

Following [**14**] again, one can prove that (u, v) is indeed a weak solution for (3.1), so that we obtain

Theorem 3.4. *The Cauchy problem* (3.1) *has a global weak solution for arbitrary initial data of bounded variation in the r, s variables.*

Remark . Since, being of bounded variation in u, v implies being of bounded variation in r, s, one may replace in the assumption of Theorem 3.4 the stronger requirement that initial data should be of bounded variation in u, v. It is important to point out that boundedness of variation in the r, s variables is the appropriate assumption. Indeed, it is this property which is preserved in the course of wave interactions, while the variation in the u, v variables may become unbounded, as a consequence of the lack of strict hyperbolicity on the line $u = v$. This is illustrated by the example following.

Example 3.5.   Assume the initial data are linearly increasing, strictly positive functions of bounded variation on **R**. On the strip $S_0 := \{(x, t) : -\infty < x < \infty\}$ the solution of each Riemann problem consists of a T-wave and a 2-shock wave. It can be shown that the variation (in x) of the approximate solution in u, v, for any fixed t, $0 < t < s$, is unbounded as $O(h^{-1/2})$ as the mesh length h approaches zero (see Figure 3.15).

4. A particular Cauchy problem and pattern differentiation.
In this section we shall consider a special initial value problem for (0.1), motivated by the equations (0.2) introduced in Section 1. Indeed, we
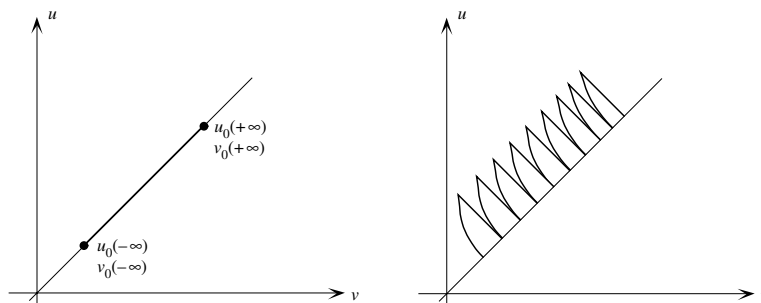
FIGURE 3.15. Unbounded variation in the (u, v)-variables.

shall consider (3.1) with the initial data

$$(4.1) \quad u_0(x) = \begin{cases} 0, & x < -a \\ u_-, & -a \le x < 0 \\ u_+, & 0 \le x < a \\ 0, & x > a, \end{cases}$$

$$v_0(x) = \begin{cases} 0, & x < -a \\ v_-, & -a \le x < 0 \\ v_+, & 0 \le x < a \\ 0, & x > a, \end{cases}$$

where a is a given positive constant, $u_\pm, v_\pm$ are given constants such that $u_- \le v_-$, $u_+ \le v_+$ (see Figure 4.1). If we choose v_-, u_- positive and v_+, u_+ negative, these data correspond to "peaks" in the U_0, V_0 quantities representing the (initial) densities of the populations U, V governed by system (0.2), see Figure 4.2.

In order to deal with the problem (0.1), (4.1), we solve the corresponding Riemann problems at $t = 0$ for $x = -a$, $x = 0$, $x = a$ first and then deal with the interaction of the associated waves. By the results of Section 2, it turns out that the solution of the Riemann problem (0.1) with initial datum $(u, v) = (0, 0)$ for $x < -a$, $(u, v) = (u_-, v_-)$ for $x > -a$ consists of a T-wave and a 2-shock emanating from the point $(-a, 0)$, denoted by $S_2(-a, 0)$. Likewise, the solution of the Riemann problem (0.1) with initial datum $(u, v) = (u_-, v_-)$ for $x < 0$,
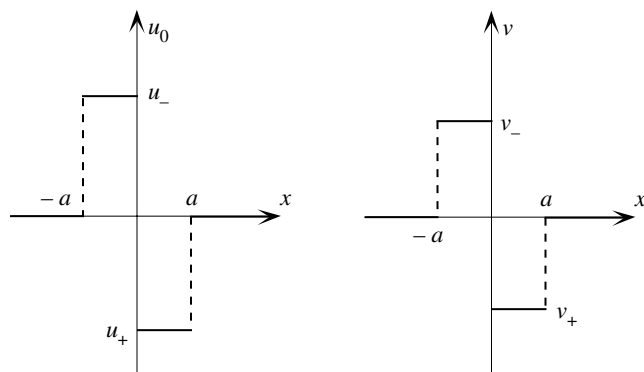
FIGURE 4.1. Special initial data for (0.1).

$(u, v) = (u_+, v_+)$ for $x > 0$, consists of a 1-shock emanating from the point $(0, 0)$, denoted by $S_1(0, 0)$ a T-wave and a 2-shock denoted by $S_2(0, 0)$. Finally, the solution of the Riemann problem (0.2) with initial datum $(u, v) = (u_+, v_+)$ for $x < a$, $(u, v) = (0, 0)$ for $x > a$, consists of a 1-shock emanating from the point $(0, 0)$, denoted by $S_1(a, 0)$ and a T-wave (see Figures 4.2 and 4.3). Clearly, the shocks $S_2(-a, 0)$ and $S_1(0, 0)$ will interact with each other, and so do the shocks $S_2(0, 0)$ and $S_1(a, 0)$. Denote, by (x_A, t_A), the coordinates in the (x, t)-plane of the point where the shocks $S_2(-a, 0)$ and $S_1(0, 0)$ meet. Then consider the Riemann problem consisting of system (0.1) supplemented, at time $t = t_A$, with data $(u, v) = (u_- + v_-, 0)$ for $x < x_A$, $(u, v) = (0, u_- + v_-)$
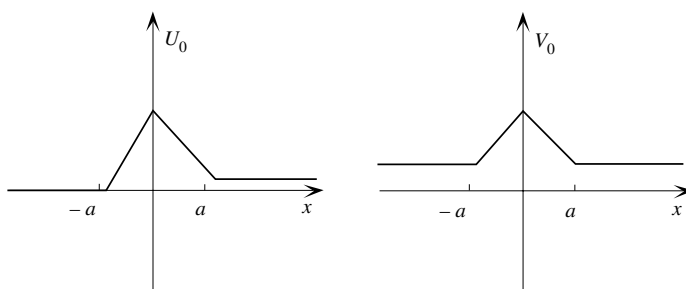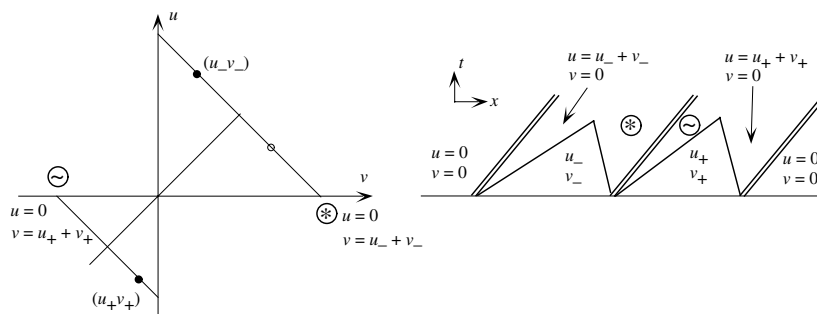

FIGURE 4.2. Corresponding initial data for system (0.2).

FIGURE 4.3. Solving Riemann problems at $x = -a$, $x = 0$, $x = a$.

for $x > x_A$. Plainly, the solution consists of a T-wave joining the states $(u = u_- + v_-, \; v = 0)$ and $(u = 0, \; v = u_- + v_-)$. Next denote, by (x_B, t_B), the coordinates where the shocks $S_2(0,0)$ and $S_1(0,a)$ meet and consider the Riemann problem consisting of system (0.1) supplemented, at time $t = t_B$, with data $(u, v) = (0, u_+ + v_+)$ for $x < x_B$, $(u, v) = (u_+ + v_+, 0)$ for $x > x_B$. Again, the solution consists of a T-wave joining the states $(u = 0, v = u_+ + v_+)$ and $(u = u_+ + v_+, v = 0)$. As a result of this analysis, it turns out that the solution of (0.1), (4.1) consists, for $t \geq \max\{t_A, t_B\}$, of five T-waves, all traveling with the speed $\sigma = 1$ (see Figure 4.4). Let us compute the values of t_A, t_B, x_A, x_B. Toward this end, observe that the speed of $S_2(-a, 0)$ is $\sigma_2 = 1 + u_-$ and that of $S_1(0,0)$ is $\sigma_1 = 1 - v_-$. Therefore,

$$t_A = a/(u_- + v_-),$$
$$x_A = a(1 - v_-)/(u_- + v_-).$$

Likewise, since the speed of $S_2(0,0)$ is $\sigma_2 = 1 - v_+$ and that of $S_1(a, 0)$ is $\sigma_1 = 1 + u_+$, we obtain

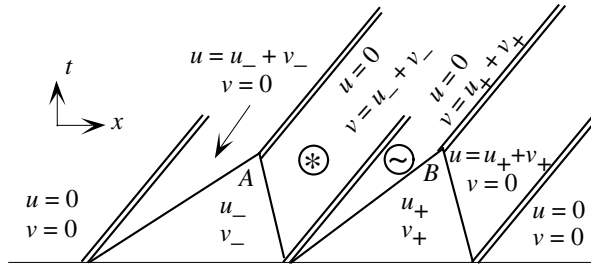$$t_B = -a/(u_+ + v_+),$$
$$x_A = -a(1 - v_+)/(u_+ + v_+).$$

FIGURE 4.4. Resulting wave patterns.

It is clear that, for $t \geq \max\{t_A, t_B\}$, v is defined as

$$v(x,t) = \begin{cases} 0, & x < x_A + (t - t_A), \\ u_- + v_-, & x_A + (t - t_A) \leq x < t, \\ u_+ + v_+, & t \leq x < x_B + (t - t_B), \\ 0, & x \geq x_B + (t - t_B), \end{cases}$$

so that $v(x, y)$ experiences three jumps, each of which propagates with speed $\sigma = 1$. Observe that the strength of jumps is larger than that of the initial jump; however, the solution's support becomes narrower, for $[x_B + (t - t_B)] - [x_A + (t - t_A)] = a[v_+/(u_+ + v_+) + v_-/(u_- + v_-)] < a$. Similarly, for $t \geq \max\{t_A, t_B\}$, u is defined as

$$u(x,t) = \begin{cases} 0, & x < t - a, \\ u_- + v_-, & t - a \leq x < x_A + t - t_A, \\ 0, & x_A + (t - t_A) \leq x < x_B + (t - t_B), \\ u_+ + v_+, & x_B + (t - t_B) \leq x < a + t, \\ 0, & x \geq a + t. \end{cases}$$

This shows that, after a finite time, the initial jump is split into two "square waves" of opposite sign, each propagating with the same speed (see Figure 4.5). From the above expressions for u, v we easily derive those for $U(x,t)$, $V(x,t)$, i.e., if we agree to define the latter quantities as the primitives (with respect to x) of $u(x,t)$, $v(x,t)$ which take, for large x's, the constant values $U_0(a)$, $V_0(a)$, respectively. Thus,
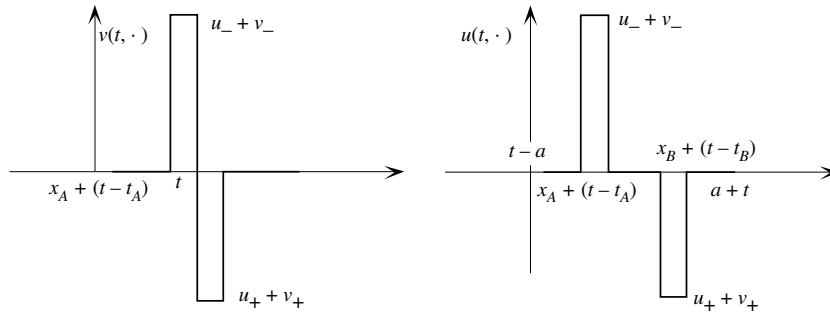
FIGURE 4.5. Wave profiles for u, v for $t \geq \max\{t_A, t_B\}$.

the initial data U_0, V_0 develop, after a finite time, into traveling wave solutions with speed $= 1$: in the moving coordinate frame $\xi = x - t$, U has a flatter profile than at time zero, while V has a steeper one (see Figure 4.6). The calculations are particularly simple in the special case $u_+ = v_+ = -\delta$, $u_- = v_- = \delta$ (where $\delta > 0$), which means that the initial profiles of both components are the same: the results are illustrated in Figure 4.7, which displays the wave profiles for (u, v), (U, V) initially and, after a time, $t^* = a(1 - \delta)/2\delta$. The same initial distribution of U, V gives rise, after a finite time, to traveling waves exhibiting a "sharp" profile for V and a "flat" profile for U. Therefore, the initial value problem considered in the present section may serve as a model for pattern formation, since the initial configuration in which
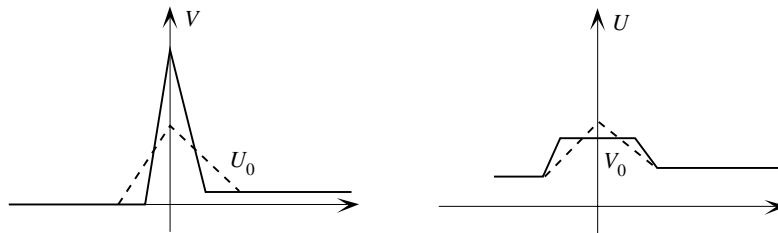

FIGURE 4.6. Profiles of $U(t, \cdot)$, $V(t, \cdot)$ for $t \geq \max\{t_A, t_B\}$ (in the moving coordinate $x - t$) compared with those of $U_0(\cdot)$, $V_0(\cdot)$.
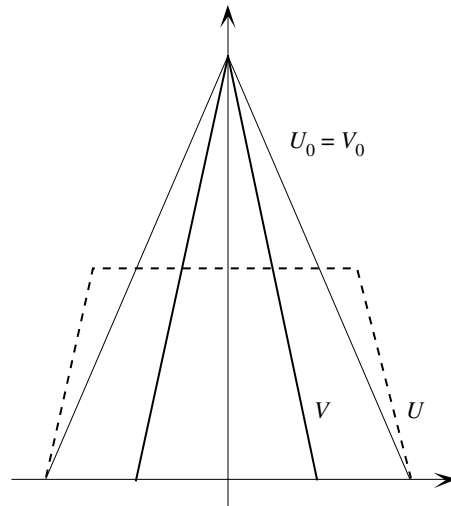
FIGURE 4.7. Wave profiles in the symmetric case:

thin line: $U_0(x) = V_0(x)$

thick lines: $U(t, x-t)$ for $t > t^*$ (dotted)

$V(t, x-t)$ for $t > t^*$ (solid).

U and V are mutually undifferentiated evolves into a permanent wave in which U and V have markedly different profiles.

REFERENCES

1. R. Aris and N. Amundson, *Mathematical methods in chemical engineering*, Vol. 2, Prentice-Hall Inc., Englewood Cliffs, NJ 1973.

2. C.M. Dafermos and L. Hsiao, *Hyperbolic systems of balance laws with inhomogeneity and dissipation*, Indiana Univ. Math. J. **31** (1982), 471–491.

3. J. Glimm, *Solutions in the large for nonlinear hyperbolic systems of equations*, Comm. Pure Appl. Math. **18** (1965), 697–715.

4. L. Hsiao and T. Chang, *Perturbation of the Riemann problem in gas dynamics*, J. Math. Anal. Appl. **79** (1981), 436–460.

5. F. Helferich and G. Klein, *Multicomponent chromatography*, Marcel Dekker Inc., New York, 1970.

6. E. Isaacson, *Global solutions of Riemann problems for a non-strictly hyperbolic system of conservation laws arising in enhanced oil recovery*, J. Comp. Phys., to appear.

7. B. Keyfitz and H. Kranzer, *A system of non-strictly hyperbolic conservation laws arising in elasticity theory*, Arch. Rat. Mech. Anal. **72** (1980).

8. P.D. Lax, *Hyperbolic systems of conservation laws* II, Comm. Pure Appl. Math. **10** (1957), 537–566.

9. ——, *Shock waves and entropy*, in *Contributions to nonlinear functional analysis* (E. Zarantonello, Ed.), Academic Press, New York, 1971, 603–634.

10. T.-P. Liu, *Approximation and qualitative behavior of admissible solutions of hyperbolic conservation laws*, Mem. Amer. Math. Soc. (1984).

11. —— and C.H. Wang, *On a hyperbolic system of conservation laws which is not strictly hyperbolic*, MRC Technical Summary Report No. 2184, Dec. 1980.

12. J.D. Murray and J.E.R. Cohen, *On nonlinear convective dispersal effects in an interacting population model*, SIAM J. Appl. Math., **43** (1983), 66–78.

13. H. Rhee, R. Aris and N.R. Amundson, *On the theory of multicomponent chromatography*, Phil. Trans. Roy. Soc. **A267** (1970), London, 419–.

14. B. Temple, *Global solutions of the Cauchy problem for a class of 2×2 non strictly hyperbolic conservation laws*, Adv. in Appl. Math. **3** (1982), 335–375.

Institute of Mathematics, Academia Sinica, Beijing, People's Republic of China

Dipartimento di Matematica, Seconda Università di Roma, Italy